JGR Space Physics

RESEARCH ARTICLE
10.1029/2019JA027197

Ionospheric Perturbations Induced by a Very Severe Cyclonic Storm (VSCS): A Case Study of Phailin VSCS

Adarsh Dube[1], Rajesh Singh[1], Ajeet K. Maurya[2], Sanjay Kumar[3], P. S. Sunil[4,5], and Abhay K. Singh[3]

[1]KSK Geomagnetic Research Laboratory, Indian Institute of Geomagnetism, Allahabad, India, [2]Department of Physics, Doon University, Dehradun, India, [3]Department of Physics, Banaras Hindu University, Varanasi, India, [4]Indian Institute of Geomagnetism, Navi Mumbai, India, [5]Department of Marine Geology and Geophysics, Cochin University of Science and Technology, Kochi, India

Key Points:
- First study from north Indian Ocean which concentrates on ionospheric perturbations associated with a very severe cyclonic storm (VSCS)
- Study uses TEC data from seven GPS station located in the impact region of VSCS Phailin which occurred during 09–13 October 2013Peak perturbation in DTEC at GPS stations is found to be maximum during VSCS in comparison with precyclone and postcyclone days

Correspondence to:
R. Singh,
rajeshsing03@gmail.com

Citation:
Dube, A., Singh, R., Maurya, A. K., Kumar, S., Sunil, P. S., & Singh, A. K. (2020). Ionospheric perturbations induced by a very severe cyclonic storm (VSCS): A case study of Phailin VSCS. *Journal of Geophysical Research: Space Physics*, *125*, e2019JA027197. https://doi.org/10.1029/2019JA027197

Received 23 JUL 2019
Accepted 14 DEC 2019
Accepted article online 26 DEC 2019

Abstract We investigate *F* region ionospheric perturbations associated with very severe cyclonic storm Phailin which occurred in Bay of Bengal during 09–12 October 2013. Very severe cyclonic storm Phailin was the most intense supercyclone over the Bay of Bengal with intensity ~T6.0. The primary data used are lightning data from Global Lightning Detection 360 network, Global Position System-derived total electron content information from seven Global Position System stations located in the cyclone impact region, and meteorological data. This is the first report from north Indian Ocean which investigates the perturbations induced in the ionosphere associated with a cyclone. Investigation of lightning discharges occurrence at the storm center along the cyclone track line showed that the lightning growth pattern closely follows the cyclone intensity during the initial, mature, and decay stages. The total electron content computed from seven Global Position System stations showed that differential total electron content is enhanced during very severe cyclonic storm days, compared with precyclone and postcyclone days. The maximum peak-to-peak perturbation in differential total electron content values at Port Blair located at Andaman-Nicobar Islands in Bay of Bengal was ~0.33 TECu during the cyclone days, whereas it was only ~0.11 TECu during the no-cyclone days. The results show that most probably gravity waves generated from cyclonic thunderstorms can couple with the upper atmosphere and modify the dynamics of the ionosphere. Tropical cyclones and large thunderstorms are an important source from below which couple with ionosphere and manifest in the form of ionospheric perturbations.

1. Introduction

A tropical cyclone is a major hazard for both human life and property, particularly in the cyclone impact region. “Cyclone” is a generic term used for a low-pressure system over tropical or subtropical regions, with organized deep convection, thunderstorm activity, and gusty winds at low levels (Holland, 1993). The distinctive feature associated with a tropical cyclone is deep convective clouds, thunderstorms, and associated high-energy lightning discharges. During last couple of decades several reports have established that atmospheric gravity waves (AGWs) generated from low-pressure cyclonic system couple with our Earth's atmosphere-ionosphere system and create perturbations/disturbances in all the *D, E*, and *F* regions of the ionosphere (e.g., Collier et al., 2006*; Inan et al., 2007;* Immel et al., 2009*;* Takahashi et al., 2009*;* Kuo & Lee, 2015*;* Lay et al., 2015). This study, which is first of its kind from north Indian Ocean sector, concentrates on study of *F* region ionospheric perturbations associated with a very severe cyclonic storm (VSCS).

Bishop et al. (2006), using data from Incoherent Scatter Radar, Ionosonde, and Global Positioning System (GPS) receivers, studied the *F* region plasma density and velocity variations above the passage of the December 2003 tropical storm Odette. The study reported large velocity variations of about 10–80 m/s in the plasma drift component during the intense phase of the cyclonic storm. Wave activity with an average periodicity of ~90 min was also reported in their results. *Perevalova et al.* (*2010*) investigated the action of several tropical cyclones in the *F* region ionosphere on the basis of measurements of variations in the total electron content (TEC) derived from the network of GPS receivers. They have suggested ionospheric disturbances such as changes in electron density concentration, temperature, and formation of irregularities in the ionosphere as the possible manifestations of tropical cyclones. In a study from the southern hemisphere, Vanina-Dart and Sharkov (2013) observed similar Ionospheric GPS TEC variations during the tropical cyclone Yasi over Australia.

There are number of reports of *F* region ionospheric perturbations due to mesoscale convective system thunderstorms, apart from cyclone-associated thunderstorms. Lay et al. (2013) reported enhanced localized fluctuations in ionospheric *F* region TEC in time and space corresponding to significant thunderstorm activity over the U.S. continental region. Anomalous perturbation in ionospheric TEC up to ~1.4 TECu during the nighttime hours is reported in their results. Shao et al. (2014) presented similar studies of *F* region TEC variations in response to lightning discharges and their parental thunderstorms. In another study by Rai et al. (2006), consistent enhancement in ion and electron temperatures were reported due to convective activity associated with localized thunderstorms. Vadas and Liu (2009) reported in a modeling study that AGWs generated by thunderstorms can lead to ionospheric TEC perturbation of about ±7%. Largely during last couple of decades, several studies on the thunderstorm from tropical cyclones and mesoscale convective system have drawn attention of the scientific community to these potential sources which can perturb ionosphere from below.

Several studies as cited studied ionospheric perturbations associated with severe weather systems across globe. But studies of characterization of electrical activity of a cyclonic storm and associated ionospheric perturbations are sparse from north Indian Ocean region. In this study which is the first of its kind from the Indian sector, we concentrate on studying the perturbations induced in the *F* region ionosphere from thunderstorm associated with a tropical cyclone. VSCS Phailin which occurred in Bay of Bengal during October 2013 has been taken up as a case study. It is always very important to have a serious statistical analysis, based on much larger number of relevant data set of cyclone and no cyclone days. Because of non-availability of various data set required to perform statistical analysis, such study will be taken up in future with more number of severe weather cases. In this case study we present a cyclone from north Indian ocean which produced *F* region perturbations during intense phase of the cyclone. Precyclone and postcyclone the ionospheric variations were observed to be normal.

To understand the energetics of how thunderstorms associated with a cyclonic storm can induce ionospheric perturbations, it is necessary to understand intense mesoscale convective system and associated lightning activity from the initial to mature stage of the cyclone. During Phailin, oceanic storm surge reached the heights of 2 m above the astronomical tide, heavy rainfall over a 24-hr cumulative rainfall reached the maximum of ~30 cm, and gale force wind gusted to ~220 kmph. The sea surface temperature, based on satellite and available buoys and ship observations, was about 28–29 °C and the ocean thermal energy was about 60–80 kJ/cm^2 as reported by the India Meteorological Department (IMD; http://www.imd.gov.in/). This laid favorable conditions for the intensification of the very severe cyclonic storm Phailin. It is important to mention that Phailin was the most intense supercyclone in the Bay of Bengal after the Odisha Supercyclone that hit the east coast of India in 1999, both in terms of intensity and in the order of time.

From the Indian sector, the study of tropical cyclones for three cases has been reported by Guha et al. (2016) where they reported a decrease in vertical TEC (VTEC) values from GPS observations on the day of landfall of the storm. But the electrical aspects of the cyclonic storm, such as characterization of strength and intensity of lightning discharges energy released associated with the cyclone time thunderstorms is lacking from the Indian ocean sector. In this investigation, efforts have been made to show that convective thunderstorm activity during a VSCS, like Phailin can influence the ionosphere in the form of perturbation from below. This is probably the first results on low-latitude ionospheric perturbation due to the effects of VSCS-associated thunderstorms over the Indian region.

The present work focuses on the role of a tropical cyclone in modifying the charge and energy balance of the upper atmosphere by studying the link between convective thunderstorm activity and their effects in the upper atmosphere-ionosphere. The data used and method of data analysis are described in sections 2 and 3, observations and discussion in sections 4 and 5, and the summary of the unique results is presented in section 6.

2. Data Set

The Phailin VSCS lasted for five days from 09–13 October 2013. To understand the genesis, development, and dissipation stages of this event we have used the services of the IMD's Regional Specialized Meteorological Centre for Tropical Cyclones over North Indian Ocean (http://www.rsmcnewdelhi.imd.gov.in). The IMD's best-track data are used to locate the movement and center (i.e., the eye of the cyclone),

Table 1
Information of GPS Stations With Their Geographical Coordinates

Serial no.	Station code	Location	Geographic latitude	Geographic longitude
01	pbri	Port Blair	11.63778	92.71214
02	sgoc	Colombo	6.89208	79.87418
03	pond	Pondicherry	12.01663	79.84891
04	visa	Vishakhapatnam	17.72492	83.32247
05	hyde	Hyderabad	17.41728	78.55088
06	iisc	Bangalore	13.02117	77.57038
07	lcki	Lucknow	26.91252	80.95592

along with the intensity of the cyclone which attained the category of T6.6 (on Dvorak's intensity scale; Dvorak, 1975). Also, the meteorological measurements for the periods of the VSCS Phailin from IMD like astronomical tide, gale wind, and rainfall are used to understand the impact of the cyclone in the Bay of Bengal.

Further, to understand the electrical nature of VSCS associated thunderstorms and resultant perturbations in the ionosphere we have used two other primary data sets. The first primary data set used is lightning data from Vaisala Inc. (https://www.vaisala.com/), the Global Lightning Detection 360 (GLD360) network data set, to get information of location, discharge polarity, and peak current radiated by lightning discharges associated with thunderstorms (Said et al., 2010*; Said* et al., 2013). GLD360 is the ground-based lightning detection network capable of providing worldwide coverage with uniform and high performance without severe detection differences between daytime and nighttime conditions (Nag et al., 2015). The expected detection efficiency and median location accuracy of GLD360 are ~70% and 5–10 km, respectively, for cloud to ground strokes.

The second primary data set used is the ionospheric TEC, estimated from the ground-based GPS measurements over equatorial and low-latitude stations located around the Bay of Bengal region which covered the spatial scale of VSCS Phailin. GPS data were obtained from four stations: Colombo (sgoc), Hyderabad (hyde), Bangalore (iisc), and Lucknow (lcki) operated by the International GNSS Service network (http://www.igs.org/network), and three local network stations at Port Blair (pbri), Pondicherry (pond), and Visakhapatnam (visa) maintained by Indian Institute of Geomagnetism (http://www.iigm.res.in/). The details of the GPS station are presented in Table 1, and Figure 1 depicts the location of GPS sites. Figure 1 also show Phailin VSCS storm track from 08–14 October 2013 and GLD360 lightning discharge activity on 11 October 2013 when the eye of the cyclone was clearly visible in the lightning occurrence plot.

3. Method of GPS-Derived TEC Analysis

Seven GPS stations were selected from International GNSS Service and Indian Institute of Geomagnetism network to cover the impact region of Phailin VSCS (Table 1 and Figure 1). The data in Receiver Independent Exchange (RINEX) format obtained from selected stations were processed to estimate ionospheric slant total electron content, and which was subsequently converted to VTEC using a mapping function described by Seemala and Valladares (2011). In this study, the VTEC data measured by suitable satellite pseudo random number (PRN) passes have been selected such that the elevation angle is >30°; in this way, close proximity of the VTEC data and thunderstorm time occurrence around GPS station is taken care of. Accordingly, PRN 32 was chosen for 09 and 10 October, and PRN 2 was chosen for 11 and 12 October 2013. The undisturbed (or background) TEC is computed using the method of fitting a best fit polynomial to the original VTEC curve. This method has been used by several workers (*e.g.,* Lay et al., 2013). The ionospheric perturbation in TEC (differential total electron content (DTEC)) is estimated by subtracting the best polynomial fitted data from the original VTEC data of the selected PRN. This process removes the gross offset, and the DTEC mainly corresponds to the phase TEC having accuracy 0.01–0.1 TECu (Burrell et al., 2009). Therefore, any perturbation with DTEC >0.1 TECu can be considered as caused by any geophysical phenomena either from above or below. Order of polynomial is chosen using method of minimised chi-square between the observations and the fit for determining the best order of the polynomial. For the curve fitting of observed TEC data at seven stations, polynomial of the order 9 was found suitable and is used in analysis.

We also checked the variation of geomagnetic indices such as *Kp* index, to identify geomagnetic disturbance during the analysis period. The *Kp* index during the VSCS Phailin was ≤4; hence, period was geomagnetically moderately quiet (http://wdc.kugi.kyoto-u.ac.jp/). Further, we also looked into solar $F_{10.7}$, extreme ultraviolet, and X-ray flux since these solar radiation are the primary source of ionospheric ionization. All three parameters for complete month of October 2013 are presented in Figure 2 (data source: https://omniweb.gsfc.nasa.gov, https://www.ngdc.noaa.gov, https://dornsife.usc.edu/space-sciences-center/download-sem-data/). First five days, that is, 01–05 October, are solar quite (Figure 2), and therefore, average of these

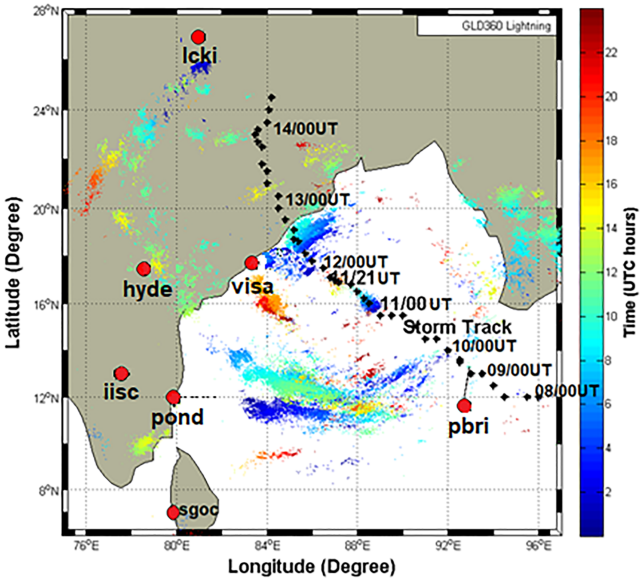

Figure 1. Location of GPS stations, storm track of the cyclone, and associated lightning activity on mature day, 11 October 2013.

five pre no cyclone days is used as the base line (blue curve) and compare with observed enhanced TEC perturbations during cyclone and postcyclone days as presented in Figures 7 and 8.

Figure 3 represents GPS data analysis method adopted as described above for the station of Port Blair (pbri). Figures 3a and 3b show the VTEC and DTEC variations over pbri station on the cyclone day of 10 October 2013 and compared with the pre no cyclone days. In Figure 3b, the blue curve is the differential TEC obtained by fitting polynomial to the TEC of the no cyclone day, whereas red curve is differential TEC of the cyclone day. Subsequently, root-mean-square error (RMSE) of the obtained DTEC is also computed and presented in Table 3. At all seven GPS stations, no cyclone day RMSE for PRN32 varied between 0.0075 and 0.0716, and PRN2 RMSE varied between 0.0050 and 0.0161. RMSE for the cyclone days at all seven GPS stations varied between 0.0013 and 0.0716. To determine the additional perturbations induced during cyclone days we also calculated the peak-to-peak magnitudes (PPM) of DTEC between no cyclone and cyclone days. PPM is peak-to-peak magnitudes or maxima of the peak-to-peak values of DTEC. The PPM values along with the RMSE is discussed in section 4.3 and presented in Table 3.

4. Observations

4.1. Phailin VSCS Intensity During 09–12 October 2013

Figure 1 depicts information of Phailin VSCS genesis, track, intensity, and rapid intensification to very severe cyclone. The genesis of VSCS Phailin which attained maximum intensity of T6.6 originated from a depression with intensity T1.5 over the Bay of Bengal on 08 October 2013. The growth to deep depression and then to a cyclonic storm did take place on 09 October 2013. Intensification to T4.0 occurred at 06:00 UTC of 10 October as the spiral bands were more organized and the eye, that is, center of cyclone, at this time was located in the middle sector of the Bay of Bengal (at ~geographic latitude 15.1°N, geographic longitude 90.6°E). The eye cloud top temperature was around −42 °C and diameter of the eye was ~12 km (http://www.rsmcnewdelhi.imd.gov.in). Moving over an area of high sea surface temperature ~28–29 °C, high ocean thermal energy 60–80 kJ/cm^2, and especially low vertical wind shear (10–15 m/s), Phailin rapidly intensified into a VSCS on the same day of 10 October 2013 (http://www.rsmcnewdelhi.imd.gov.in). It stayed over the open water on 11 October 2013 and grew to an intensity of more than T6.0. After its landfall near Gopalpur, Odisha (geographic latitude 19.26°N, geographic longitude 84.82°E) at 16:00 UTC on 12 October 2013, it finally decayed into a well-marked low-pressure area over eastern India on the following days. On 12 October 2013 the eye of the cyclone was within range of IMD's Vishakhapatnam station Doppler Weather Radar (geographic latitude 17.44°N, geographic longitude 83.20°E). Figures 4a–4d present Doppler Weather Radar imagery on 12 October 2013 for the period from 10:59 to 18:00 UTC. The eye of VSCS is marked with a red circle in Figure 4. Based on Vishakhapatnam Doppler Weather Radar observations, features of the eye and the position of the VSCS Phailin on 12 October are listed in Table 2.

4.2. Lightning Discharge Distribution Around Storm Center of VSCS Phailin

The focus of the present study is to understand perturbations induced in the *F* region ionosphere by thunderstorm associated with VSCS Phailin. Since lightning discharges are inevitably related with a convective thunderstorm activity, we have used lightning discharge data to understand the electrical nature of thunderstorms associated with VSCS Phailn. First we attempted to understand the distribution of lightning discharge in and around the storm center or eye of the cyclone within a 100-km diameter during the period 09–13 October 2013. The geolocation of the storm center at 3-hourly intervals is taken from the IMD report and is depicted as storm track centers in Figure 1. The temporal evolution of lightning discharges at the center of the storm track, that is, cyclone eye during 09–13 October 2013, is presented in Figure 5 along with sea level pressure, wind speed, and distribution of lightning discharges. Figure 5a shows the decrease in sea level

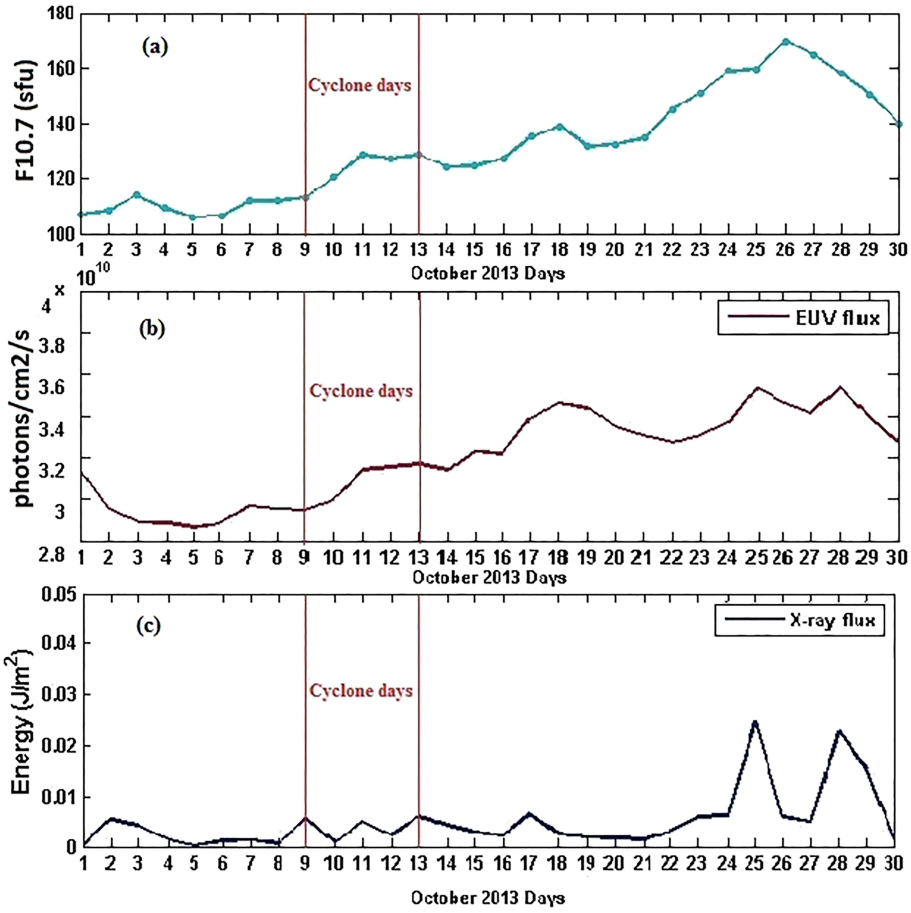

Figure 2. Solar activity indexes $F_{10.7}$, EUV, and X-ray flux for the month of October 2013.

pressure (marked with blue dots) and the gradual increase in wind speed (marked with green dots). With ~1,000-hPa pressure and ~15-m/s wind on 09 October, at 09:00 UTC, Phailin evolved into a cyclone and on 10 October, at 06:00 UTC, with ~990-hPa pressure and ~30-m/s wind, it further evolved in to a VSCS. It is important to note that during VSCS phase of Phailin, on 10 October and first half of 11 October saturation in both sea level pressure (~941 hPa) and wind speed (~60 m/s) was observed.

Figure 5b shows the distribution of total number of lightning discharges and polarity (+/−) in the cloud-to-ground (CG) lightning discharges in storm center of the cyclone during the period 09–13 October. The blue colored bars are the total number of lightning discharges around the storm center of the cyclone. Red bars represent the number of +CG lightning discharges, whereas black bars represent the number of −CG lightning discharges. It can be noticed that during VSCS phase on 10 and first half of 11 October maximum number of lightning were observed, and the +CG and −CG discharges have almost equal distribution. Further it is evident from Figure 5b that the growth of associated lightning discharges at the center of VSCS is similar to the growth pattern of the intensity of the cyclone as described above in section 4.1. The initial day of convection on 09 October produced fewer lightning discharges at the storm center when compared with the intense cyclone days from 09−12 October 2013. The final days after 12 October during the decay of the cyclone, the storm center saw very little lightning activity (0.15% of the total duration). Figure 5c shows the peak current distribution of the lightning discharges. The distribution of peak current with time shown in Figure 5c is displayed using 3 hr by 30-kA bins. The investigation of lightning discharge along storm track provided the basic understanding of the lightning discharges in eye of the cyclone from its genesis to VSCS category and subsequent dissipation. Subsequently, the GPS stations were selected to cover the impact region of VSCS Phailin to understand the perturbations induced in the ionosphere due to cyclone time thunderstorms, and is presented subsequently in next section.

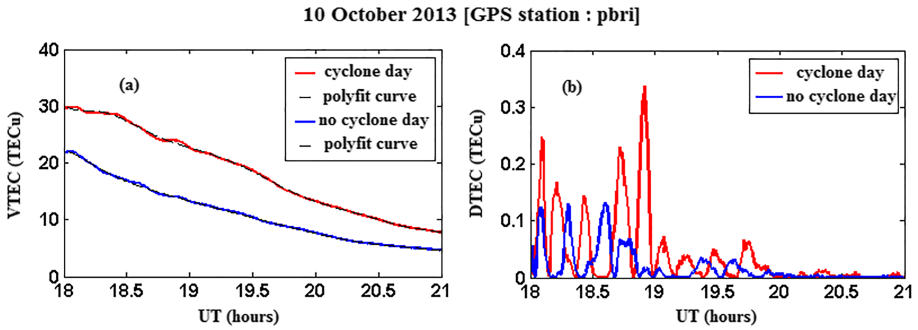

Figure 3. (a) TEC variations along with best polynomial fit to it over pbri station during 1800–2100 UTC, on 10 October 2013. (b) DTEC values from the gross offset of the best fit.

4.3. *F* Region Ionospheric Perturbations During, Pre-, and Post-VSCS Phailin

Figures 6a–6d show lightning activity associated with thunderstorms during 09–12 October Phailin VSCS days in the impact region (geographic latitude 05–30°N, geographic longitude 75–96°E). The selected region includes the location of seven GPS stations (pbri, pond, visa, sgoc, iisc, hyde, lcki). Figure 6 also depicts Ionospheric Pierce Point (the path of the signal transmitted from the satellite to the receiver where it crosses the ionospheric shell) paths of selected PRN32 and PRN2 during cyclone days of 09–12 October 2013. Color bars at the bottom on the respective subplots in Figures 6a–6d represent the passage time of PRNs in UTC. It can be noticed that Ionospheric Pierce Point paths of PRN32 and PRN2 as observed from all GPS stations is under heavy impact of lightning discharges during 09–12 October. The blue color circles (300-km radius) around the GPS stations in Figures 6a–6d depict the lightning activity. Enhanced lightning flashes indicate strong convective thunderstorm activity, which is likely the source of generation of AGWs responsible for observed ionospheric perturbation from below.

On 09 and 10 October it can be observed that lightning activity was high and uniformly spread over all GPS stations during a 24-hr period except for the station of lcki. Minimal lightning activity was observed on all four days of the cyclone at lcki. 11 October was the day when eye of the cyclone was clearly visible and lightning activity was organized with spiral rain bands of the VSCS. Consequently, on 11 October lightning activity was almost minimal at stations of lcki, iisc, pond, pbri, and sgoc. Whereas the stations of hyde and visa were under the influence of heavy lightning activity. On 12 October when VSCS Phailin made landfall, the cyclone was still intense with organized spiral rain bands associated lightning discharges. The stations of lcki, iisc, pond, pbri, and sgoc again saw minimal lightning activity on 12 October. The associated DTEC perturbations due to the cyclone time thunderstorm activity at respective GPS stations are discussed and presented next in Figure 7. Postcyclone DTEC variations are presented in Figure 8.

Figure 7 shows DTEC variations over seven GPS stations during the no cyclone and cyclone period. 09 and 10 October uses TEC data of PRN32, and 11 and 12 October uses PRN2 satellite pass data. In Figure 7 (all four vertical panels), the blue curve represents variations in DTEC during no cyclone days. No cyclone day (blue curve) DTEC values presented are after the data analysis method described in section 3, except for sgoc because of unavailability of data. For sgoc, the no cyclone days chosen are 15–18 October. Care is taken that no cyclone days (01–05 October) do not have any significant disturbance from Sun to perturb the ionosphere from above. The red curve in all panels of Figure 7 shows the DTEC variations during respective cyclone days of 09–12 October. On 09 October there were no data available at the stations of visa, and on 10 October no data at visa and hyde. The example plot, to estimate DTEC, is shown as Figure 3a, which depicts the VTEC variation observed from PRN 32 over pbri station on 10 October 2013. The deviation in VTEC, that is, DTEC curve, is obtained by subtracting the fitted data from the original VTEC data as shown in Figure 3b.

From Figure 7, it can be observed that enhancement in TEC variations is prominent over those stations that are close to the region of enhanced lightning activity thunderstorms (within 300 km blue circle drawn over GPS stations in Figure 6). GPS stations are chosen so that they cover the impact region of cyclone, and also with reference to center of the cyclone track starting from geographic latitude 12°N

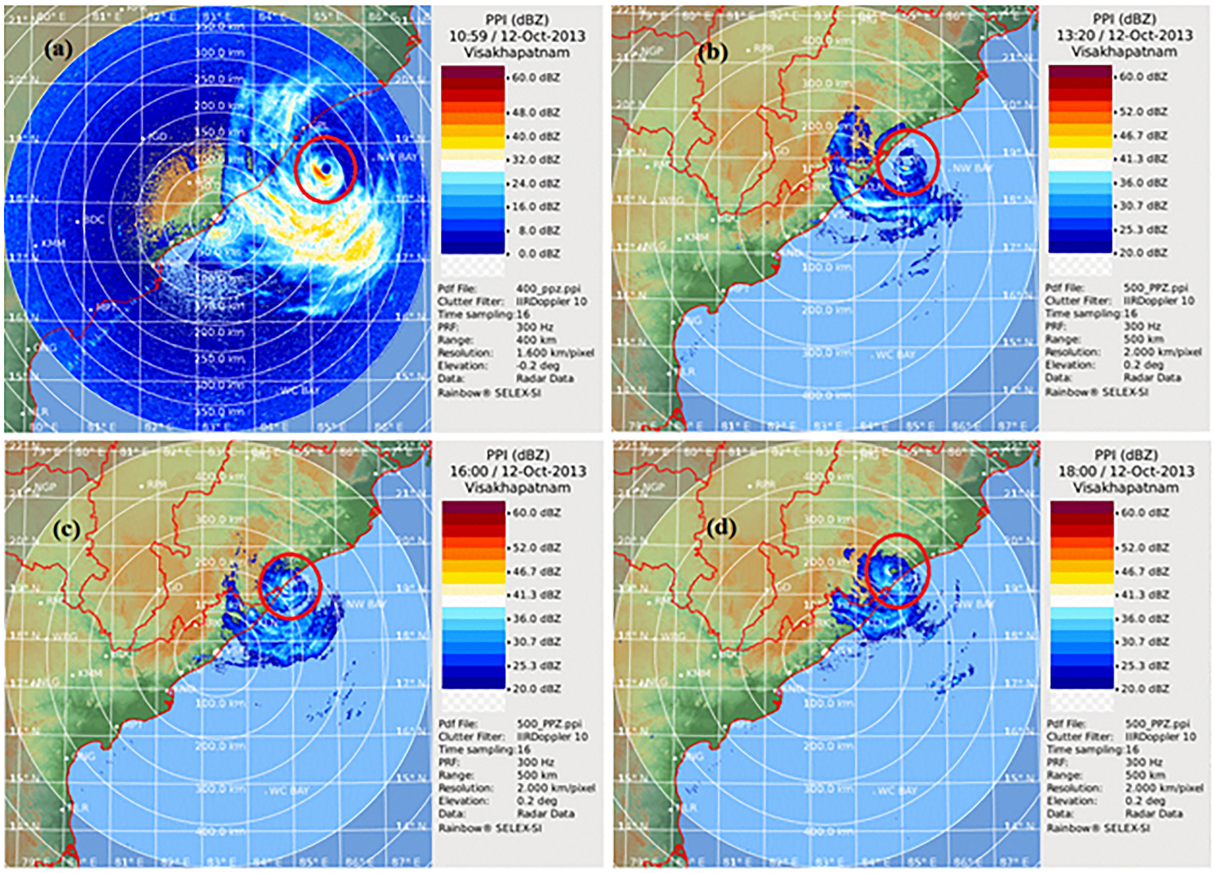

Figure 4. (a–d) Doppler Weather Radar (DWR) imageries of Phailin on 12 October 2013 as observed from DWR installed by IMD at Vishakhapatnam (17.72°N, 83.32°E), India (source: http://www.imd.gov.in/).

and geographic longitude 96°E, up to geographic latitude 24.5°N and geographic longitude 84.5°E. Lowest latitude of all the GPS stations is ~6°N for Colombo (sgoc) and highest geolatitude is of Lucknow (lcki), that is, ~26°N.

When the center of the cyclone was lying in the Bay of Bengal in the latitude 13–15°N and longitude 89–94°E on 09 and 10 October, the enhancements in VTEC variation are evident in GPS stations with location around latitude 6–17°N and longitude 77–92°E. The stations which saw enhanced TEC perturbations on 09 were iisc, pond, and pbri (Figure 7). We cannot comment for the station at visa because of nonavailability of data. On 10 October again the stations of pond, iisc, and pbri saw enhanced perturbations. There were no data available for the station visa and hyde on 10 October. As the cyclone moved northwestward on 11 and 12

Table 2
Features of the Eye and Position of the VSCS Phailin on 12 October 2013 Based on DWR, Vishakhapatnam (17.72°N, 83.32°E), India (Source: http://www.imd.gov.in/)

Serial no.	Date and time (UTC)	Latitude (°N)	Longitude (°E)	Range (kms)	Azimuth (°)	Radial wind speed (mps)/eye diameter (km)	Shape of eye and confidence
1	12/10/2013 0120Z	17.647	86.258	309	91.5	-/NA	Almost closed eye, fair
2	12/10/2013 0350Z	17.912	85.899	270	85.6	-/36.5 km	Almost closed eye, good
3	12/10/2013 0600Z	18.058	85.734	255	81.7	40/30.0 km	Almost closed eye, good
4	12/10/2013 1100Z	18.599	85.261	223	64.7	58/26.0 km	Almost closed eye, good
5	12/10/2013 1410Z	18.997	85.094	231	52.8	60/18.0 km	Almost closed eye, good
6	12/10/2013 1635Z	19.282	84.934	238	44.1	45/16.0 km	Eye over land, good
7	12/10/2013 1725Z	19.415	84.853	243	40.5	42/NA	Eye over land, fair

NA = not available.

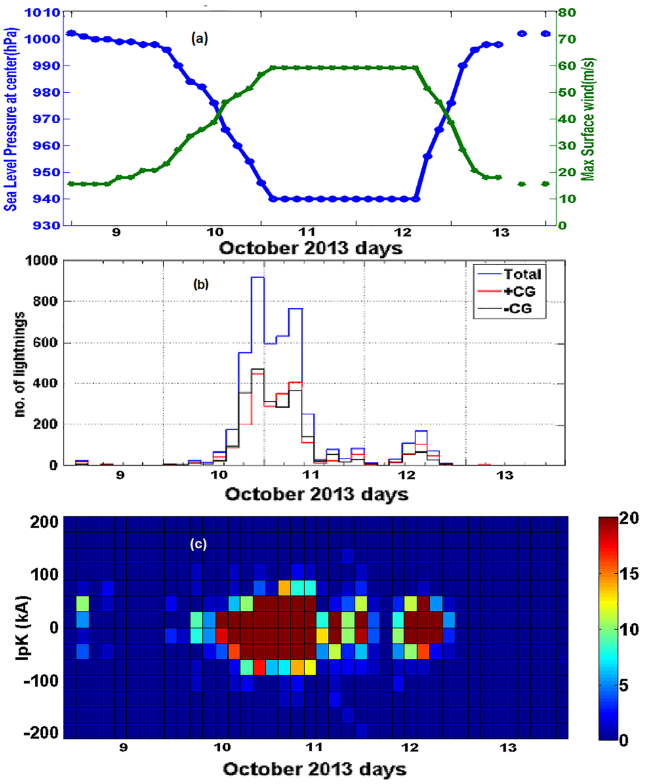

Figure 5. Temporal evolution of inner core lightning in VSCS Phailin. (a) Maximum sustained winds (in green squares) and minimum central pressure (blue circles). (b) Lightning activity within 100 km of storm center binned in 3-hr intervals (black bars are negative CG lightning, red bars are positive CG lightning, and blue bars are the total number of lightning discharges. (c) Spectrogram of peak currents (I_{pk}) using 3 hr by 30-kA bins. The color bar indicates the number of lightning events in each bin and dark red represents 10 or more events.

October, the impact seems to reduce in the TEC perturbation at pond, iisc, pbri, and sgoc on 11 and 12 October (Figure 7). As the cyclone moved further northwestward, enhanced perturbations can be seen over visa and hyde (Figure 7) on the landfall day of 12 October. The station of lucknow (lcki) and colombo (sgoc) were located away from the main cyclone impact region, and hence, we could not observe any enhancement in DTEC on no-cyclone and cyclone days. Next we present Figure 8 which shows DTEC variations during postcyclone days of 13–16 October. The blue curve in Figures 7 and 8 is average of solar quiet (Figure 2) five precyclone days (01–05 October), and is used as the baseline to compared with enhanced TEC perturbations during cyclone and postcyclone days. It can be observed in Figure 8 that both blue and red curves are almost following same variations after the dissipation of VSCS Phailin. Hence, the enhanced *F* region ionospheric perturbations were only observed during cyclone days, whereas the precyclone and postcyclone variations were normal.

The PPM of differential TEC observed for no cyclone days (blue color) and cyclone days (red color) as presented in Figure 7 are listed in Table 3. PPM is peak-to-peak magnitudes or maxima of the peak-to-peak values of DTEC presented in Figure 7. Please note that on no cyclone days PPM values were very less, in the range of ~0.0032–0.11 TECu. At the station of lucknow (lcki) and colombo (sgoc) located in least cyclone impact region the PPM values were almost comparable on cyclone and no cyclone days. During the cyclone days of 09–12 October, the PPM values were enhanced in cyclone impact region GPS stations of visa, hyde, pond, iisc, and pbri. PPM at these stations were in the range of ~0.0177–0.3370 TECu. On 09 when VSCS Phailin was in the Bay of Bengal, the PPM at pbri was 0.2543 TECu. During entire VSCS period it was on 10 October when maximum PPM of 0.3370 TECu was observed at pbri. When cyclone was approaching costal mainland, PPM at iisc was 0.1130 TECu on 10 October. Subsequently, during 11–12 October when VSCS had a landfall near visa station, the enhancement in PPM was observed at visa and hyde. On 11 October the PPM at vsia was 0.0396 TECu, and on landfall day of 12 October the value was 0.1598 TECu. Subsequently, the cyclone weakened during 13–16 October and no perturbation in DTEC was observed as shown in Figure 8. Figures 7 and 8 and Table 3 clearly show that during the VSCS days of 09–12 October enhancement in DTEC was observed when compared with precyclone and postcyclone days. The most plausible explanation of the enhanced DTEC seem to be acoustic-gravity waves generated by thunderstorm and this is discussed in the next section.

5. Discussions

The primary aim of the present report is to understand the perturbations induced in the ionosphere due to thunderstorms associated with a tropical cyclone in the Indian sector. Among several studies reported on ionospheric perturbations associated with severe weather system such as thunderstorms, cyclone, hurricane, and typhoon, one such study from the Indian subcontinent is absent till now and present report aims to perform such study. In a previous study using the database of 45 hurricanes and lightning discharge detection from the space-based Tropical Rainfall Measurement Mission (TRMM) satellite, Cecil et al. (2002) reported that the inner core of a tropical cyclone is least likely to produce major lightning activity. But our study which uses lightning discharge data from ground-based sensors shows significant discharges from the inner core of a tropical cyclone along the storm track as presented in Figure 5. In the 100-km radius from storm center the total number of CG lightning discharges reached ~1,000 counts on 10 October 2013 during the cyclone. It is important to mention that the detection efficiency of the GLD360 network is around ~70%

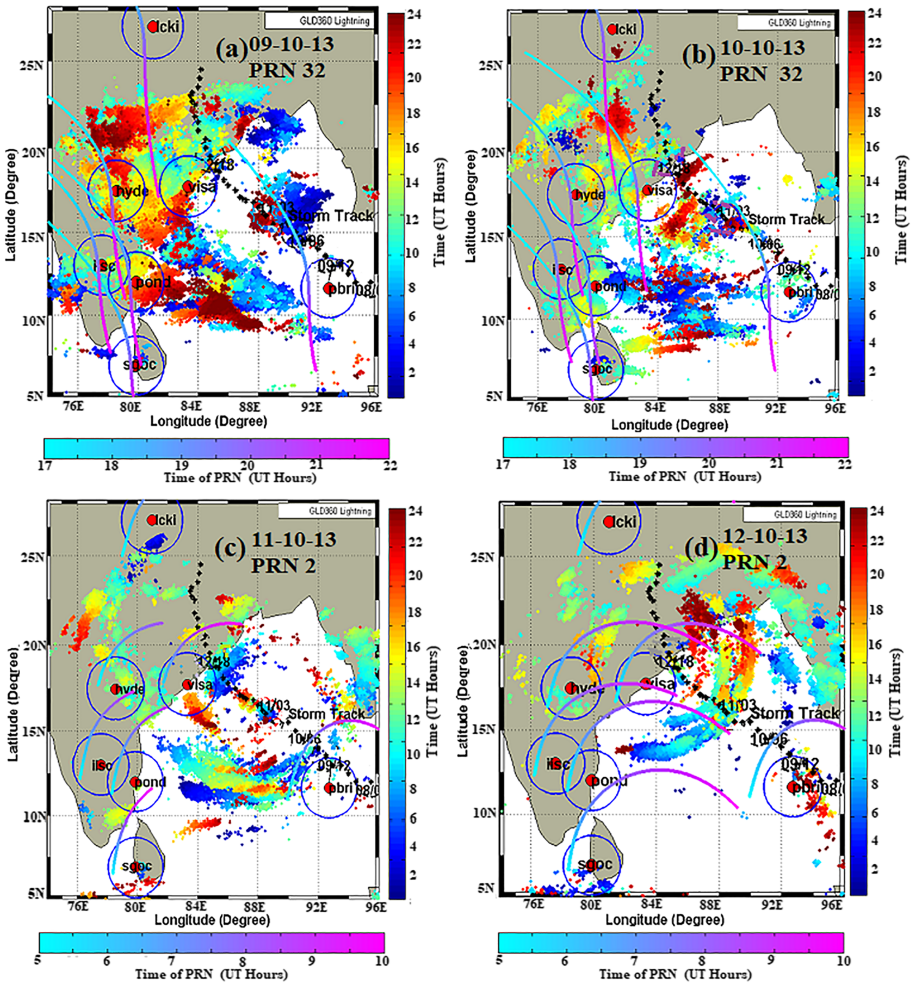

Figure 6. (a–d) GLD360 lightning discharges during the intensification of Phailin cyclone from 09 to 12 October 2013, cyclone best track, location of the GPS stations that falls under the cyclone's total impact area, and path of IPP over respective station. The blue color circles with radius of 300 km around the GPS stations depict the lightning activity around station.

and hence there maybe be more discharges in the storm center. Further the GLD360 recorded lightning discharges shows that inner core is endowed with a large number of high-energy lightning discharges with peak current in the range of ±200 kA which is sufficient to drive ionospheric perturbations.

Demaria et al. (2012) investigated the tropical cyclone cases from the Atlantic and eastern North Pacific Oceans and reported that tropical cyclones tend to have more lightning density than the hurricanes. They also showed that the lightning density during the intensification of the storm is greater than during the weakening or dissipating phase. Another study by Zhang et al. (2012) on the tropical cyclones making landfall in China suggested that the lightning outbreak from the eye wall region (within the inner core) can be a potential indicator for storm intensification. The present work further corroborates the important role of inner core lightning as the indicator of storm intensification. Phailin rapidly intensified into a VSCS of category T6.0 on 10 October 2013 when the lightning discharges in the eye of storm center reached maximum counts (Figure 5c). Hence, previous reports and our observations suggest that the real-time coverage of lightning strikes at storm center can be useful for better forecasting results in prediction of the intensification of tropical cyclones. The uniqueness of the present report is that all of the previous studies cover cyclones across the globe, other than north Indian Ocean. Hence, this study is an important contribution from the Indian subcontinent.

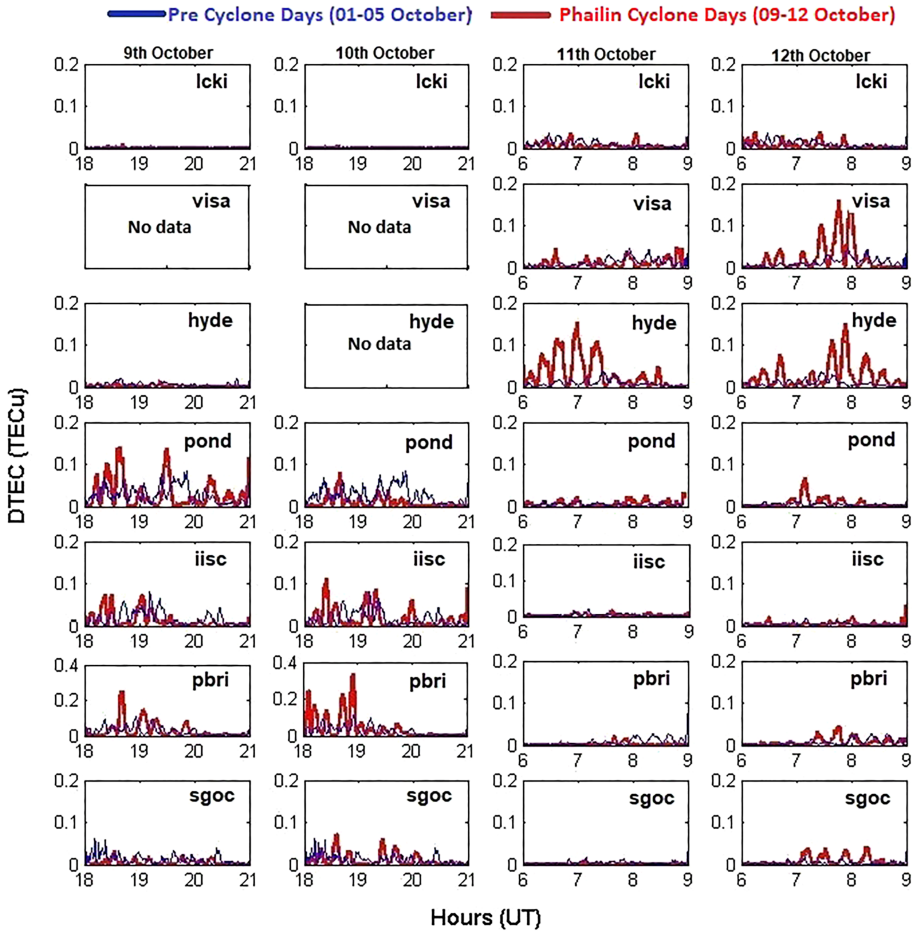

Figure 7. Precyclone (01–05 October) and VSCS Pahilin days (09–12 October 2013) DTEC variations over GPS stations (precyclone days, blue curve is 01–05 October average DTEC).

VSCS Phailin associated *F* region ionospheric perturbations over the Bay of Bengal during the period from 09 to 12 October 2013 are studied in detail in this report for the ionospheric variation pre, during, and post periods of cyclone. Perturbations in DTEC computed over seven GPS stations are shown in Figures 7 and 8. It is observed that perturbations in DTEC have been noticed over all GPS stations, with a maximum PPM value of 0.3370 TECu. Vadas and Liu (2009) reported ~ 2 TECu deviation in DTEC for deep convection from Brazil and have suggested that TEC deviation is probably caused by gravity waves (GWs) generated by convective plumes. Recently, using the data from GPS-based measurements, Lay et al. (2013) studied the influence of deep convective thunderstorms on ionospheric perturbations and reported the maximum deviation up to ~1.4 TECu. In all the reports for ionospheric perturbations due to thunderstorms, the primary mechanism proposed is due to the generation of GWs. The period of thunderstorm induced GWs range from 30 to 180 min have been reported by previous workers (e.g., Hocke & Schlegel, 1996; Bishop et al., 2006; Oliver et al., 1997). Immel et al. (2009) reported signatures of atmospheric tides generated from tropospheric weather systems and proposed that tides can transport the tropospheric energy to the edge of space and modify the ionosphere.

Model results of acoustic gravity wave propagation are consistent with several reported observations, and indicate that such waves originating from thunderstorm heights (<12 km) should be able to reach 250–350-km altitude within ~250 km horizontally of the source (e.g.,Walterscheid et al., 2003; Zettergren & Snively, 2013). *Zettergren et al.* (2013) in their numerical simulation with one wave source in the southern hemisphere and another wave source in northern hemisphere have demonstrated that a

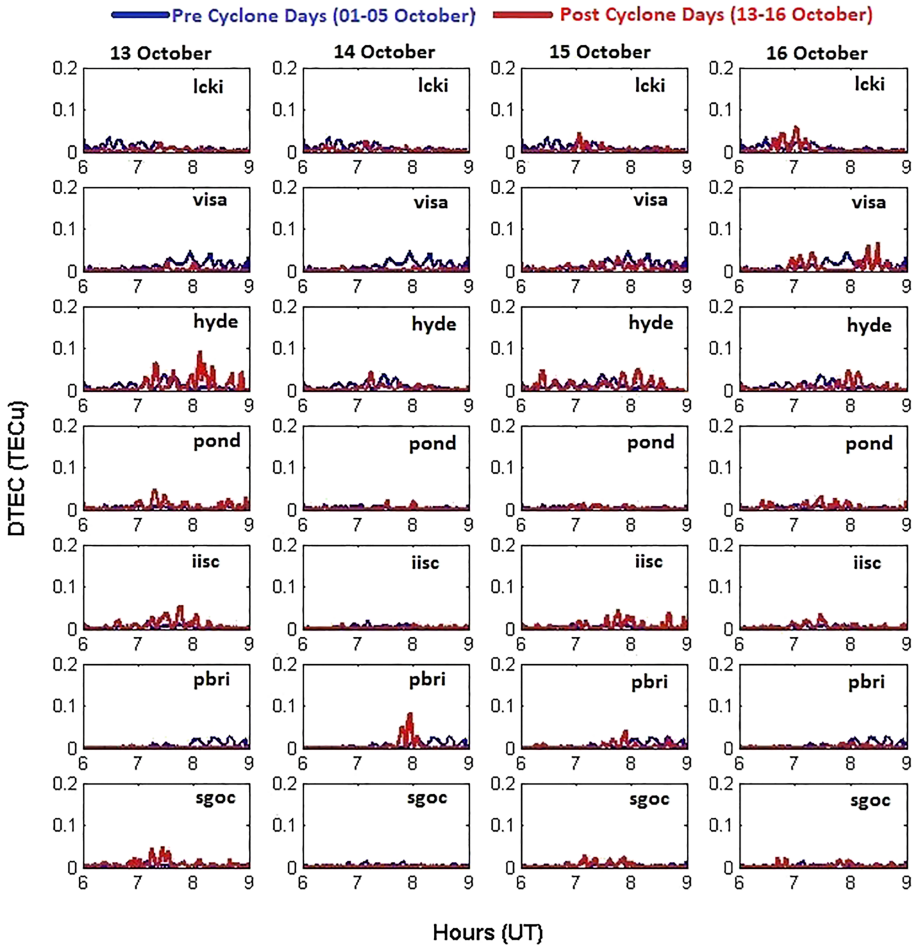

Figure 8. Precyclone (01–05 October) and post-VSCS Phailin days (13–16 October 2013) DTEC variations over GPS stations (precyclone days, blue curve is 01–05 October average DTEC).

simple tropospheric updraft produces TEC responses in the ionosphere which is observable via GPS stations. In another study from South America using optical instruments at four different locations Takahashi et al. (2009) showed that GWs generated in the tropospheric convective regions propagate upward at a slant angle through the mesosphere and thermosphere and can reach up to the bottom side of *F* layer ionosphere. The GWs are able to reach up to 100–220 km in altitude, and can produce a perturbation in the *F* layer of the ionosphere by changing the plasma density and modulating the electric field (Bishop et al., 2006). Further Weather Research and Forecasting model simulations made by Pathakoti et al. (2016) strongly support the presence of Stratosphere-Troposphere mixing during severe cyclones. The possible linkage of the likely phenomena such as thunderstorms, cyclones, and earthquakes that occur within the limits of Earth surface and the tropospheric boundary to the upper atmospheric region of Ionosphere is also examined in the studies of infrasound waves associated with these phenomena (Chum et al., 2018; Georges, 1973; Jones & Georges, 1976). These studies stand for evidence that besides the gravity waves, also infrasound waves cause perturbations in the ionosphere just above the large convective cells and tropical cyclones.

Our results on *F* layer ionospheric perturbation during 09–12 October 2013 Phailin VSCS shows that TEC perturbations are enhanced during cyclone days in comparison with precyclone and postcyclone days The plausible reason as discussed seems to be because of the GWs generated in tropospheric convective regions, and propagated in the slant direction toward the ionosphere (Abdu et al., 2009). This possible mechanism of gravity waves generated by thunderstorms during VSCS Phailin that propagated in a slant direction and

Table 3
Peak-to-Peak Magnitudes (PPM) of DTEC as Observed From the GPS Stations

GPS stations	9 October 2013 PPM (RMSE)	10 October 2013 PPM (RMSE)	No cyclone day (PRN32) PPM (RMSE)	11 October 2013 PPM (RMSE)	12 October 2013 PPM (RMSE)	No cyclone day (PRN2) PPM (RMSE)
lcki	0.0098 (0.0014)	0.0052 (0.0013)	0.0033 (0.0716)	0.0359 (0.0086)	0.0396 (0.0104)	0.0032 (0.0127)
visa	No data	No data	No data	0.0396 (0.0104)	0.1598 (0.0402)	0.0469 (0.0161)
hyde	0.0200 (0.0035)	No data	0.0215 (0.0075)	0.1532 (0.0467)	0.1503 (0.0380)	0.0371 (0.0120)
pond	0.1407 (0.0432)	0.0808 (0.0146)	0.0827 (0.0337)	0.0333 (0.0086)	0.0696 (0.0128)	0.0272 (0.0056)
iisc	0.0745 (0.0211)	0.1130 (0.0283)	0.0615 (0.0245)	0.0177 (0.0043)	0.0501 (0.0067)	0.0187 (0.0050)
pbri	0.2543 (0.0502)	0.3370 (0.0716)	0.1100 (0.0362)	0.0207 (0.0041)	0.0522 (0.0117)	0.0148 (0.0109)
sgoc	0.0490 (0.0082)	0.0726 (0.0177)	0.0602 (0.0168)	0.0089 (0.0016)	0.0442 (0.0128)	0.0288 (0.0054)

Note. Table also includes root-mean-square error (RMSE) values of DTEC.

reached the heights of the ionosphere and thereby creating variations in *F* region TEC only during cyclone period seems to explain observations of enhanced DTEC at all GPS stations, except at lucknow (lcki) which is located away from cyclone impact region.

Apart from this, the generation of electrical current due to thunderstorm activity also plays a significant role in producing the ionospheric perturbation. Recently, using a thunderstorm model, Kuo and Lee (2015) have shown that the thunderstorm-induced current propagates upward and can reach into the ionosphere. As we do not have any electric field measurements for this study of VSCS Phailin, we cannot comment on this aspect of the mechanism of perturbation. In addition, a chain of lightning discharges occurring during a long-lasting thunderstorm activity during the VSCS period could cause significant variations in the conductivity in the regions above it, and can cause the electron density variations in the middle ionosphere (e.g., Vellinov et al., 1992b; Pasko et al., 1997).

6. Summary

In the present study, thunderstorm-induced perturbation in *F* region ionosphere associated with the VSCS Phailin during 09–12 October 2013 is described. The work is the first of its kind from the north Indian Ocean region on VSCS. Enhanced ionospheric variations in GPS-TEC observations, elaborated as DTEC variations (Figure 7) at GPS stations located in the cyclone impact region are observed during cyclone days only. Precyclone and postcyclone scenario shows that ionospheric variation was normal (Figure 8). We summarize our unique findings on north Indian Ocean VSCS induced ionospheric perturbations as below:

1. The analysis of inner core suggest that the inner core of the tropical cyclones can have increased lightning activity, unlike earlier studies reported with less lightning in the inner core of hurricanes, and typhoons of Atlantic and Pacific Ocean origin. Further it is observed that the inner core is endowed with a large number of high-energy lightning discharges with peak current in the range of $\pm$200 kA.
2. Thunderstorm-induced variations in the ionosphere are clear from the observations of enhanced TEC variations over five GPS stations located in the impact region during cyclone days only (Figure 7). Precyclone and postcyclone TEC variations were found to be normal (Figure 8). The PPM variation in DTEC during cyclone days was in the range of ~0.0177–0.3370 TECu. In comparison, PPM values during no cyclone days were ~0.0032–0.11 TECu. The Port Blair (pbri) station located in Bay of Bengal observed maximum PPM value of ~0.3370 TECu.

The exact mechanism of thunderstorm-induced ionospheric perturbation is not clear even today due to many factors which influence the ionosphere simultaneously. Some possible mechanisms are generation of AGWs when thunderstorm overshoot the upper part of the troposphere, that is, tropopause (Vadas & Liu, 2009), modification in electric field by thunderstorm activity (Bishop et al., 2006), and formation of density bubbles by thunderstorms or thunderstorms triggering of the Perkins instability (Kuo & Lee, 2015). Therefore, since the north Indian Ocean is the region where intense severe tropical cyclones happen very frequently, further investigation by taking into consideration more cyclone cases is required and will be

taken up to resolve and understand complex atmosphere-ionosphere coupling processes from intense tropospheric cloud convective systems.

Acknowledgments
The authors would like to extend gratitude to Director, Indian Institute of Geomagnetism, for providing necessary support and encouragement to carry out research at the Institute. International GNSS team is acknowledged for the five GPS station data used downloaded from the website: ftp://cddis.gsfc.nasa.gov/pub/gps. Port Blair, Pondicherry, and Visakhapatnam GPS stations are being operated by Indian Institute of Geomagnetism (IIG) stations (http://www.iigm.res.in/), and the data can be obtained for collaborative research purpose. The Indian Meteorological Department (IMD; http://www.imd.gov.in) is acknowledged for the best track cyclone data, Doppler Weather Radar (DWR) report from Visakhapatnam station, and other meteorological measurements of VSCS Pahilin. The source of geomagnetic conditions is taken from http://www.spaceweather.com/ and http://wdc.kugi.kyoto-u.ac.jp/. Solar flux data are used from https://omniweb.gsfc.nasa.gov; https://www.ngdc.noaa.gov and https://dornsife.usc.edu/space-sciences-center/download-sem-data/. The authors acknowledge Vaisala Inc. (https://www.vaisala.com) for providing the GLD360 lightning data. Authors also thank Morris B. Cohen, Georgia Institute of Technology, Atlanta GA, USA, for the GLD360 data and support for the work carried out. A. K.M. thanks Science and Education Research Board for financial support under Ramanujan Fellowship (file no. SB/S2/RJN-052/2016) and Faculty Recharge Program (FRP) of University Grant Commission (UGC; ID FRP62343), New Delhi.

References

Abdu, M. A., Kherani, E. A., Batista, I. S., de Paula, E. R., Fritts, D. C., & Sobral, J. H. A. (2009). Gravity wave initiation of equatorial spread *F*/plasma bubble irregularities based on observational data from the SpreadFEx campaign. *Annales Geophysicae*, *27*(7), 2607–2622. https://doi.org/10.5194/angeo-27-2607-2009

Bishop, R. L., Aponte, N., Earle, G. D., Sulzer, M., Larsen, M. F., & Peng, G. S. (2006). Arecibo observations of ionospheric perturbations associated with the passage of Tropical Storm Odette. *Journal of Geophysical Research*, *111*, 1, A11320–9. https://doi.org/10.1029/2006JA011668

Burrell, A. G., Bonito, N. A., & Carrano, C. S. (2009). Total electron content processing from GPS observations to facilitate ionospheric modeling. *GPS Solutions*, *13*(2), 83–95. https://doi.org/10.1007/s10291-008-0102-3

Cecil, D. J., Zipser, E. J., Nesbitt, S. W., et al. (2002). Reflectivity, ice scattering, and lightning characteristics of hurricane eyewalls and rainbands. *Monthly Weather Review, American Meteorological Society*, *130*(4), 769–784. https://doi.org/10.1175/1520-0493(2002)130<0769:RISALC>2.0.CO;2

Chum, J., J.-Y. Liu, K. Podolská, T. Šindelářová (2018), Infrasound in the ionosphere from earthquakes and typhoons, *Journal of Atmospheric and Solar - Terrestrial Physics*, *171*, 72-82, doi:/10.1016/j.jastp.2017.07.022

Collier, A. B., Hughes, A. R. W., Lichtenberger, J., & Steinbach, P. (2006). Seasonal and diurnal variation of lightning activity over southern Africa and correlation with European whistler observations. *Annales Geophysicae*, *24*(2), 529–542. https://doi.org/10.5194/angeo-24-529-2006

Demaria, M., Demaria, R. T., Knaff, J. A., & Molenar, D. (2012). Tropical cyclone intensity and rapid intensity change. *Monthly weather review, American Meteorological Society, Volume*, *140*, 1828–1842. https://doi.org/10.1175/MWR-D-11-00236.1

Dvorak, V. F. (1975). Tropical cyclone intensity analysis and forecasting from satellite imagery. *Monthly weather review, American Meteorological Society*, May, 1975, *103*, 420–430. https://doi.org/10.1175/1520-0493(1975)103<0420:TCIAAF>2.0.CO;2

Georges, T. M. (1973). Infrasound from convective storms: Examining the evidence. *Reviews of Geophysics and Space Physics*, *11*(3), 571–594. https://doi.org/10.1029/RG011i003p00571

Guha, A., Paul, B., Chakraborty, M., & De, B. K. (2016). Tropical cyclone effects on the equatorial ionosphere: First result from the Indian sector. *Journal of Geophysical Research: Space Physics*, *121*, 5764–5777. https://doi.org/10.1002/2016JA022363

Hocke, K., & Schlegel, K. (1996). A review of atmospheric gravity waves and travelling ionospheric disturbances: 1982–1995. *Annales Geophysicae*, *14*(9), 917–940. https://doi.org/10.1007/s00585-996-0917-6

Holland, G. J. (1993). Ready Reckoner: Chapter 9, Global guide to tropical cyclone forecasting, WMO/TC-No. 560, Report No. TCP-31. In *World Meteorological Organization* (Chap. 9). Geneva, Switzerland: World Meteorological Organization (WMO).

Immel, T. J., Mende, S. B., Hagan, M. E., Kinter, P. M., & England, S. L. (2009). Evidence of tropospheric effects on the ionosphere. *Eos, Transactions of the American Geophysical Union*, *90*(9), 69. https://doi.org/10.1029/2009EO090001

Jones, R. M., & Georges, T. M. (1976). Infrasound from convective storms. III. Propagation to the ionosphere. *The Journal of the Acoustical Society of America*, *59*(4), 765–779. https://doi.org/10.1121/1.380942

Kuo, C. L., & Lee, L. C. (2015). Ionospheric plasma dynamics and instability caused by upward currents above thunderstorms. *Journal of Geophysical Research: Space Physics*, *120*, 3240–3253. https://doi.org/10.1002/2014JA020767

Lay, E. H., Shao, X. M., & Carrano, C. S. (2013). Variation in total electron content above large thunderstorms. *Geophysical Research Letters*, *40*, 1945–1949. https://doi.org/10.1002/grl.50499

Lay, E. H., Shao, X.-M., Kendrick, A. K., & Carrano, C. S. (2015). Ionospheric acoustic and gravity waves associated with midlatitude thunderstorms. *Journal of Geophysical Research: Space Physics*, *120*, 6010–6020. https://doi.org/10.1002/2015JA021334

Nag, A., Murphy, M. J., Schulz, W., & Cummins, K. L. (2015). Lightning locating systems: Insights on characteristics and validation techniques. *Earth and Space Science*, *2*(4), 65–93. https://doi.org/10.1002/2014EA000051

Oliver, W. L., Otsuka, Y., Sato, M., Takami, T., & Fukao, S. (1997). A climatology of *F* region gravity wave propagation over the middle and upper atmosphere radar. *Journal of Geophysical Research*, *102*(A7), 14,499–14,512. https://doi.org/10.1029/97JA00491

Pasko, V. P., Inan, U. S., Bell, T. F., & Taranenko, Y. N. (1997). Sprites produced by quasi-electrostatic heating and ionization in the lower ionosphere. *Journal of Geophysical Research*, *102*(A3), 4529–4561. https://doi.org/10.1029/96JA03528

Pathakoti, M., Sujatha, P., Karri, S. R., Sai Krishn, S. V. S., Rao, P. V. N., Dutt, C. B. S., & Dadhwal, V. K. (2016). Evidence of stratosphere–troposphere exchange during severe cyclones: A case study over Bay of Bengal, India. *Geomatics, Natural Hazards and Risk*, *7*(6), 1816–1823. https://doi.org/10.1080/19475705.2016.1155502

Rai, J., Sharma, D.K., Chand, R., Suda, K., & Israil, M. (2006). Effect of active thunderstorms on ionospheric electron and ion temperatures as obtained by the SROSS-C2 satellite measurements. *1st International Lightning Meteorology Conference*, 26–27 April, Tucson, arizona, USA.

Said, R. K., Cohen, M. B., & Inan, U. S. (2013). Highly intense lightning over the oceans: Estimated peak currents from global GLD360 observations. *Journal of Geophysical Research: Atmospheres*, *118*, 6905–6915. https://doi.org/10.1002/jgrd.50508

Said, R. K., Inan, U. S., & Cummins, K. L. (2010). Long range lightning geolocation using a VLF radio atmospheric waveform bank. *Journal of Geophysical Research*, *115*, D23108. https://doi.org/10.1029/2010JD013863

Seemala, G. K., & Valladares, C. E. (2011). Statistics of total electron content depletions observed over the South American continent for the year 2008. *Radio Science*, *46*, RS5019. https://doi.org/10.1029/2011RS004722

Shao, Xuan-Min., Lay, E., & Jacobson, A. (2014). Ionospheric variations in response to lightning discharges and their parental thunderstorms. *XV International Conference on Atmospheric Electricity*, 15–20 June 2014, Norman, Oklahoma, U.S.A.

Takahashi, H., Taylor, M. J., Pautet, P. D., Medeiros, A. F., Gobbi, D., Wrasse, C. M., et al. (2009). Simultaneous observation of ionospheric plasma bubbles and mesospheric gravity waves during the SpreadFEx Campaign. *Annales Geophysicae*, *27*(4), 1477–1487. https://doi.org/10.5194/angeo-27-1477-2009

Vadas, S. L., & Liu, H. L. (2009). Generation of large-scale gravity waves and neutral winds in the thermosphere from the dissipation of convectively generated gravity waves. *Journal of Geophysical Research*, *114*, 1–25. https://doi.org/10.1029/2009JA014108

Vanina-Dart, L. B., & Sharkov, E. A. (2013). Investigations into the tropical cyclone: Ionosphere interaction. *EMS Annual Meeting*, Vol. 10, EMS2013-348, 2013, 13th EMS/11th ECAM.

Vellinov, P., Spassov, C., & Kolev, S. (1992). Ionospheric effects of lightning during the increasing part of solar cycle 22. *Journal of Atmospheric and Terrestrial Physics*, *54*(10), 1347–1353. https://doi.org/10.1016/0021-9169(92)90044-L

Walterscheid, R. L., Schubert, G., & Brinkman, D. G. (2003). Acoustic waves in the upper mesosphere and lower thermosphere generated by deep tropical convection. *Journal of Geophysical Research*, *108*(A11), 1392. https://doi.org/10.1029/2003JA010065

Zettergren, M. D., & Snively, J. B. (2013). Ionospheric signatures of acoustic waves generated by transient tropospheric forcing. *Geophysical Research Letters*, *40*, 5345–5349. https://doi.org/10.1002/2013GL058018

Zhang, W., Zhang, Y., Zheng, D., & Zhou, X. (2012). Lightning distribution and eyewall outbreaks in tropical cyclones. *Monthly Weather Review, American Meteorological Society*, *140*, 3573–3586. https://doi.org/10.1175/MWR-D-11-00347.1